The EMBO Journal (2006) 25, 798–810 | © 2006 European Molecular Biology Organization | All Rights Reserved 0261-4189/06
www.embojournal.org

THE EMBO JOURNAL

A hyper-dynamic equilibrium between promoter-bound and nucleoplasmic dimers controls NF-κB-dependent gene activity

Daniela Bosisio[1,6,7], Ivan Marazzi[1,6], Alessandra Agresti[2,6], Noriaki Shimizu[3], Marco E Bianchi[4,*] and Gioacchino Natoli[5,*]

[1]Institute for Research in Biomedicine, Bellinzona, Switzerland, [2]San Raffaele Scientific Institute, Milan, Italy, [3]Faculty of Integrated Arts and Sciences, Hiroshima University, Hiroshima, Japan, [4]San Raffaele University, Milan, Italy and [5]European Institute of Oncology, Milan, Italy

Because of its very high affinity for DNA, NF-κB is believed to make long-lasting contacts with cognate sites and to be essential for the nucleation of very stable enhanceosomes. However, the kinetic properties of NF-κB interaction with cognate sites *in vivo* are unknown. Here, we show that in living cells NF-κB is immobilized onto high-affinity binding sites only transiently, and that complete NF-κB turnover on active chromatin occurs in less than 30 s. Therefore, promoter-bound NF-κB is in dynamic equilibrium with nucleoplasmic dimers; promoter occupancy and transcriptional activity oscillate synchronously with nucleoplasmic NF-κB and independently of promoter occupancy by other sequence-specific transcription factors. These data indicate that changes in the nuclear concentration of NF-κB directly impact on promoter function and that promoters sample nucleoplasmic levels of NF-κB over a timescale of seconds, thus rapidly re-tuning their activity. We propose a revision of the enhanceosome concept in this dynamic framework.

The EMBO Journal (2006) **25,** 798–810. doi:10.1038/sj.emboj.7600977; Published online 9 February 2006
Subject Categories: chromatin & transcription
Keywords: enhanceosome; kinetic microscopy; NF-κB; Rel; transcription

Introduction

After degradation of their cytoplasmic inhibitors (IκBs), the homo- and hetero-dimers composed of the five NF-κB/Rel proteins (p65/RelA, c-Rel, RelB, p50 and p52) (Thanos and Maniatis, 1995a; Verma *et al*, 1995; Ghosh *et al*, 1998) translocate to the nucleus and bind thousands of 9–10 nt κB sites dispersed in the genome (Martone *et al*, 2003; Natoli *et al*, 2005) in order to activate transcription of 200–300 genes implicated in inflammation, immune response and antiapoptosis. Mechanistic understanding of NF-κB-regulated transcription requires the definition of the kinetic properties of NF-κB interaction with this large number of sites.

In vitro results indicate that in comparison with most transcription factors (TFs) (whose affinity for cognate sites is generally close to 10^{-9} M), NF-κB dimers have a very high affinity for κB sites (from 10^{-13} to 10^{-10} M) (Urban and Baeuerle, 1990; Chen-Park *et al*, 2002), and generate very stable complexes with a half-life of 45 min (Zabel and Baeuerle, 1990). NF-κB–DNA complexes are further stabilized by cooperative protein–protein interactions with other sequence-specific TFs and architectural proteins, giving rise to multimolecular protein–DNA complexes called enhanceosomes. *In vitro* the interferon beta (IFN-β) enhanceosome (Maniatis *et al*, 1998) remains completely stable for over 10 h (Yie *et al*, 1999), but the existence of stable transcription complexes containing NF-κB *in vivo* remains to be proven.

Here, we carried out an *in vivo* kinetic and quantitative analysis of NF-κB activation, recruitment to and persistence on target genes, and transcriptional induction. We found that NF-κB association with target sites contained within transcriptionally active genes results in its *transient immobilization*, that is, a measurable reduction in mobility as compared to the nucleoplasmic NF-κB molecules. Such transient immobilization generates a window of opportunity during which encounter with partner TFs and recruitment of the transcriptional machinery must occur for transcription to start. This window of opportunity is, however, very short: *complete* turnover of NF-κB on activated chromatin occurs in less than 30 s. The fast dynamics of NF-κB binding and unbinding generates a dynamic equilibrium between promoter-bound and nucleoplasmic NF-κB dimers: cyclic oscillations in the nucleoplasmic pool of NF-κB induce parallel oscillations in promoter occupancy and transcriptional activity, which are dissociated from the occupancy of the same promoter by other TFs.

Taken together, these data indicate that NF-κB and the TFs interacting with adjacent binding sites do not generate *stable* enhanceosomes, but rather undergo short and individual interactions with their respective binding sites. Thus, the enhanceosome can be considered a well-defined set of molecular species, but a hyperdynamic one: each molecular species is represented inside the enhanceosome by individual molecules that belong to it for a very short time.

*Corresponding authors: ME Bianchi, San Raffaele University, Via Olgettina 58, 20132, Milan, Italy. Tel.: +39 02 26434 763; Fax: +39 02 26434 861; E-mail: bianchi.marco@hsr.it or G Natoli, Department of Experimental Oncology, European Institute of Oncology, Via Ripamonti 435, 20141, Milan, Italy. Tel.: +39 02 5748 9953; Fax: +39 02 5748 9851; E-mail: gioacchino.natoli@ifom-ieo-campus.it
[6]These authors contributed equally to this work
[7]Present address: General Pathology and Immunology, University of Brescia, Viale Europa 11, Brescia, Italy

Received: 26 July 2005; accepted: 19 December 2005; published online: 9 February 2006

Results

Mobility of nucleoplasmic NF-κB

We first used fluorescence recovery after photobleaching (FRAP) to analyze the average mobility of nucleoplasmic GFP-tagged NF-κB dimers. The GFP tag did not affect the ability of p65 to bind endogenous genes and to activate their transcription, indicating that this fusion protein is fully functional (Supplementary Figure S1). Because the kinetic properties of a given protein are similar among several different cell types (Phair *et al*, 2004b), we chose HeLa cells for ease of transfection.

In tumor necrosis factor (TNF)-stimulated HeLa cells, p65-GFP showed very rapid recovery kinetics, even faster than that of GR (Figure 1A and B), which is known to turn over rapidly on its binding sites (McNally *et al*, 2000). The high nuclear mobility of p65 cannot be accounted for by overexpression, as p65-GFP represents only a fraction of endogenous p65 (on average, about 50%; data not shown); moreover, cells expressing low and high levels of fluorescence, and therefore with lower and higher levels of endogenous plus transfected p65, had similar FRAP recovery kinetics (data not shown).

For comparison, we tested the mobility of a mutant p65-GFP with an about 1000-fold lower affinity for canonical κB sites (p65 23Y>A; 26 E>D) (Saccani *et al*, 2004; G Ghosh, personal communication). Mutant p65-GFP showed a FRAP recovery curve substantially faster than those of wild-type (wt) p65-GFP and of GFP-GR (Figure 1A and B) but much slower than that of GFP alone (Figure 1B), indicating that mutant p65 still interacts with chromatin.

We also performed similar FRAP experiments in HeLa cells cotransfected with p65-GFP and p50, and therefore expressing a p50/p65-GFP heterodimer. The results were similar to those obtained with the p65 homodimer: the wt p50/p65-GFP heterodimer has a fast recovery curve, and the heterodimer containing the mutated p65-GFP has an even faster one (Figure 1C).

These results are consistent with the idea that the measured kinetics of wt p65 is dominated by the binding to high-affinity sites, which may exceed 10–14 000 in mammalian genomes (Martone *et al*, 2003; discussed in Natoli *et al*, 2005).

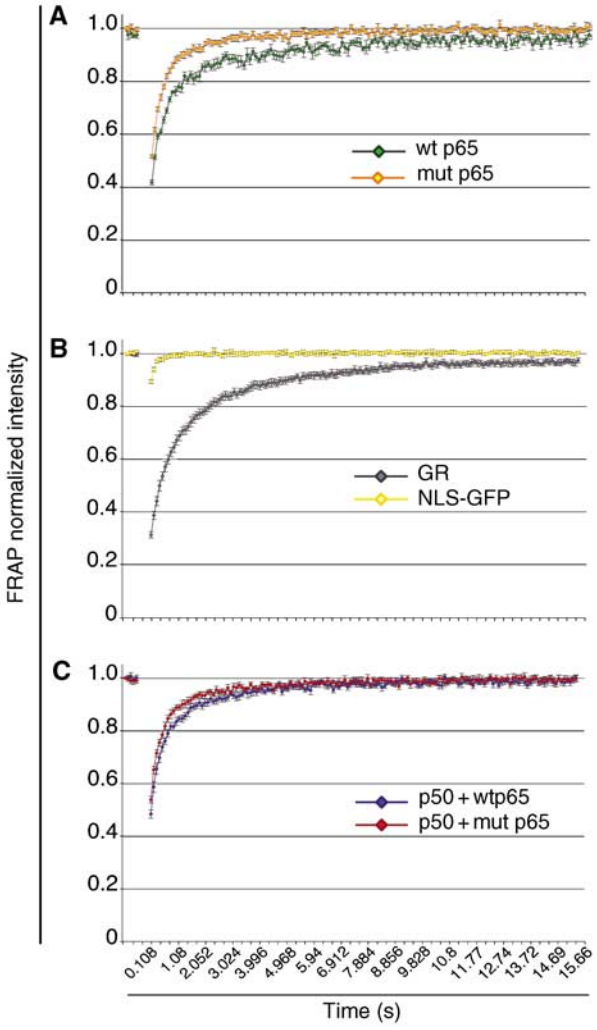

Figure 1 Evaluation of p65/RelA nuclear mobility in living cells. All curves were averaged from 15 cells each; bars represent standard error. (**A**) FRAP analysis of GFP-wt p65 and of a GFP fusion with a mutant p65 that does not bind κB sites. GFP-p65 is cytoplasmic in >95% of HeLa cells before TNF treatment (data not shown). FRAP analysis was started 20 min after TNF stimulation. The difference between the wt and mutant p65-GFP curves is statistically highly significant ($P<0.0001$). (**B**) FRAP analysis of GFP-GR (in cells treated with dexamethasone for 20′) and of a nuclear GFP (NLS-GFP) (Bonaldi *et al*, 2003). (**C**) Quantitative analysis of FRAP in cells coexpressing p50 and GFP-wt p65 or GFP-mut p65. The difference between the two curves is significant ($P<0.05$) in the first 3 s.

Rapid p65/RelA exchange on cognate binding sites in vivo

To further prove the specific binding of GFP-tagged NF-κB species to high-affinity κB sites, we constructed an array of 384 canonical κB sites (Figure 2A) and stably transfected it into HeLa cells. In many cells belonging to several different clones, a bright spot of about 1.5 μm in diameter was evident after transfection with p50/p65-GFP; similar spots were never observed in control cells. A representative nucleus containing one such cluster, and three other clusters from different clones, are shown in Figure 2B. Clearly, a high concentration of κB sites produces a high local concentration of fluorescent p65-GFP molecules.

We next measured FRAP recovery curves. Recovery on the arrays of κB sites was slower than on surrounding chromatin (Figure 2C and D), suggesting that NF-κB is immobilized onto high-affinity sites for longer than onto average genomic sequences, which contain κB sites with a wide range of affinities. Nonetheless, recovery was fast in absolute terms even on arrayed κB sites: In all, 50% recovery occurred in less than 1 s and 80% recovery was observed in about 5 s. Fluorescence on the 384 κB sites did not recover completely within 15 s, whereas fluorescence in other areas of the nucleus did. There are two most likely explanations for this behavior: a high probability of recapture of bleached NF-κB molecules dissociating from the tightly clustered κB sites, or the presence of an immobile fraction of NF-κB molecules.

To distinguish between these two possibilities, we used a modified fluorescence loss in photobleaching (FLIP) protocol. More than 90% of the nucleus (excluding the array or a control area) was repeatedly bleached (red area in Figure 2E),

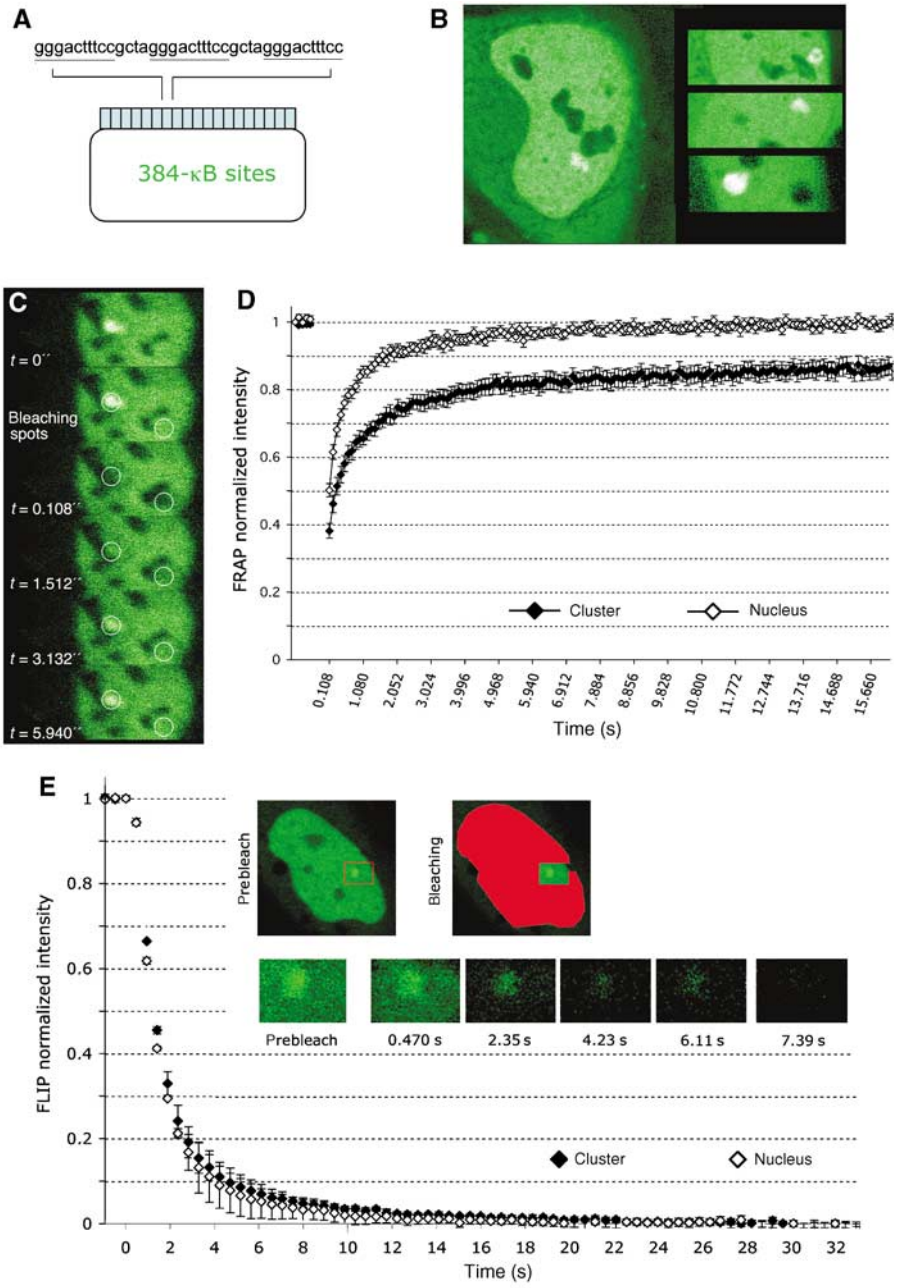

Figure 2 NF-κB binding to high-affinity κB sites in living cells. (**A**) Schematic representation of the 384-κB construct, containing 128 repetitions of a basic unit of three tandem κB sites. (**B**) Visualization of an array of 384 κB sites in living cells. Cells bearing the 384-κB construct were cotransfected with p50 and GFP-p65, stimulated with TNF for 20 min, and viewed with a confocal microscope. Four representative nuclei (from different clones) are shown. (**C**) Selected FRAP images showing bleaching and recovery of one κB site array and a different area in the nucleus (encircled). (**D**) FRAP curves for p50/p65-GFP averaged from 15 nondescript areas in the nucleus ('nucleus') and eight 384 κB site arrays ('cluster'). Bars represent standard error. (**E**) FLIP analysis of NF-κB exchange on the κB site array. A representative nucleus is shown before and after the design of the bleach area (red). The image series shows the fluorescence loss from the array over time. FLIP curves (generated as described in Supplementary Figure S2) are averaged from seven 384 κB site arrays and 15 nondescript areas in the nucleus. Bars represent standard error. The difference between the two curves is statistically nonsignificant.

and fluorescence loss from the array (or the control area) into the bleached area was measured (Figure 2E). Fluorescent molecules on the array remain fluorescent if they do not move, whereas those leaving the array are bleached as soon as they enter the area targeted by the laser. In these conditions, even a minute amount of fluorescent molecules remaining stably bound to the cluster should stand out clearly. Differently from FRAP, which is affected by both the association and dissociation rates, our modified FLIP is intended to measure the dissociation rate of fluorescent molecules from the array. Some loss of fluorescence is due to photobleaching inherent in repeated imaging of the nucleus: we corrected for this effect as shown in Supplementary Figure S2. Even after correction, analysis of the curve and the errors (Supplementary Figure S3) indicated that less than 1% of NF-κB molecules remain on the cluster after 20 s.

These results indicate that the maximal residence time of NF-κB on high-affinity sites *in vivo* is less than 20 s; this residence time is not much different from that on average chromatin, suggesting once again that NF-κB mobility in average chromatin is dominated by interactions with high-affinity sites.

NF-κB turnover on transcriptionally functional promoters

The array of κB sites is artificial and, most important, not transcriptionally active. We then set out to measure the kinetics of NF-κB exchange at arrays of transcriptionally active NF-κB-dependent genes.

We constructed a basic unit consisting of the human immunodeficiency virus (HIV) 5′ long terminal repeat (LTR), which contains two canonical κB sites, cloned upstream of a reporter gene encoding a cyan fluorescent protein (CFP) directed to peroxysomes via a C-terminal SKL tripeptide (Figure 3A). This NF-κB-responsive gene unit was cloned into the pSFV-dhfr vector. This plasmid contains both a mammalian replication initiation origin and a matrix attachment region from the Chinese hamster *dhfr* gene: when integrated into the genome, it initiates events similar to gene amplification in cancer cells, and it generates tandem repeats of up to 10 000 copies (Shimizu *et al*, 2001). We obtained arrays of several hundred plasmid copies in immortalized fibroblasts lacking both the p50 and p65 NF-κB subunits. Clone 2.24 was estimated by real-time polymerase chain reaction (PCR) to bear a repeat made of almost 2000 plasmid units (Supplementary Figure S4). After transfection of p65 and p50, TNF stimulation enhanced transcription of the CFP-SKL genes, as indicated by the increased CFP mRNA levels (Figure 3B), thus demonstrating that the array is transcriptionally active and NF-κB-regulated. Under the same conditions, HA-tagged p65 was efficiently recruited on the array, as shown by an anti-HA chromatin immunoprecipitation (ChIP) (Figure 3C). The HIV-CFP-SKL array was readily visualized upon TNF stimulation of cells reconstituted with untagged p50 and p65 tagged with monomeric red fluorescent protein (mRFP) (Figure 3D, left), although it was much less bright than the 384-κB site array (indicating a comparatively low density of κB sites). The morphology of the clusters varied from diffused (Figure 3D, top line) to beaded structures (bottom line), and was similar to the morphology of actively transcribed chromosome fibers and GR-responsive MMTV clusters (Muller *et al*, 2004).

In response to TNF stimulation, the HIV-CFP-SKL array recruited RNA-Pol II (GFP-RpbI) with a pattern that extensively overlapped the one generated by mRFP-p65 (Figure 3D, left), indicating that NF-κB recruitment coincides with productive transcription (or at least with the assembly of a preinitiation complex).

FRAP on the gene array showed 80% recovery in less than 3 s, and apparently complete recovery in about 30 s (Figure 4A). Recovery was anyway slower than that measured in the nucleoplasm, suggesting a *transient* immobilization of p65 on the array. The modified FLIP protocol described in the preceding section showed that the rate of NF-κB loss from the array was detectably smaller than the

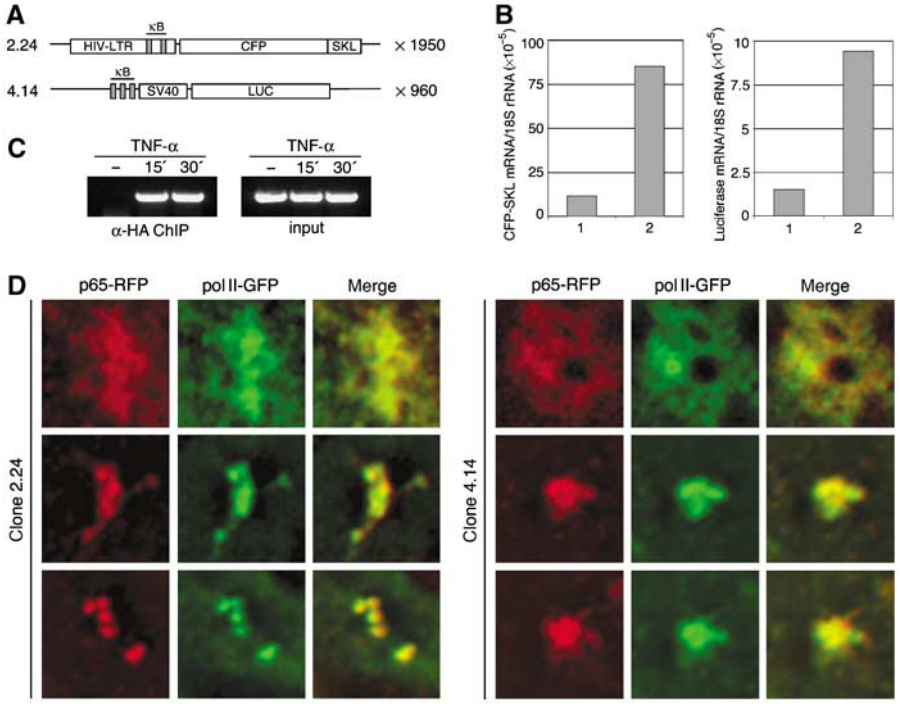

Figure 3 An array of transcriptionally functional NF-κB-regulated gene units. (**A**) Schematic representation of the NF-κB-regulated gene units amplified in clones 2.24 and 4.14. (**B**) NF-κB-dependent induction of CFP-SKL and luciferase mRNA. Clones 2.24 and 4.14 were transfected with p65 and left untreated (lanes '1') or stimulated with TNF-α for 1 h (lanes '2'). (**C**) Anti-HA-p65 ChIP on the HIV-LTR-CFP-SKL array. Clone 2.24 was transfected with HA-p65 + p50 and stimulated with TNF-α for 15′ or 30′ as indicated. (**D**) Clones 2.24 and 4.14 were transfected with mRFP-p65 and GFP-rpbI; cells were stimulated with TNF for 30′ and analyzed *in vitro*. Details of representative nuclei are shown, in which the arrays display a different morphology.

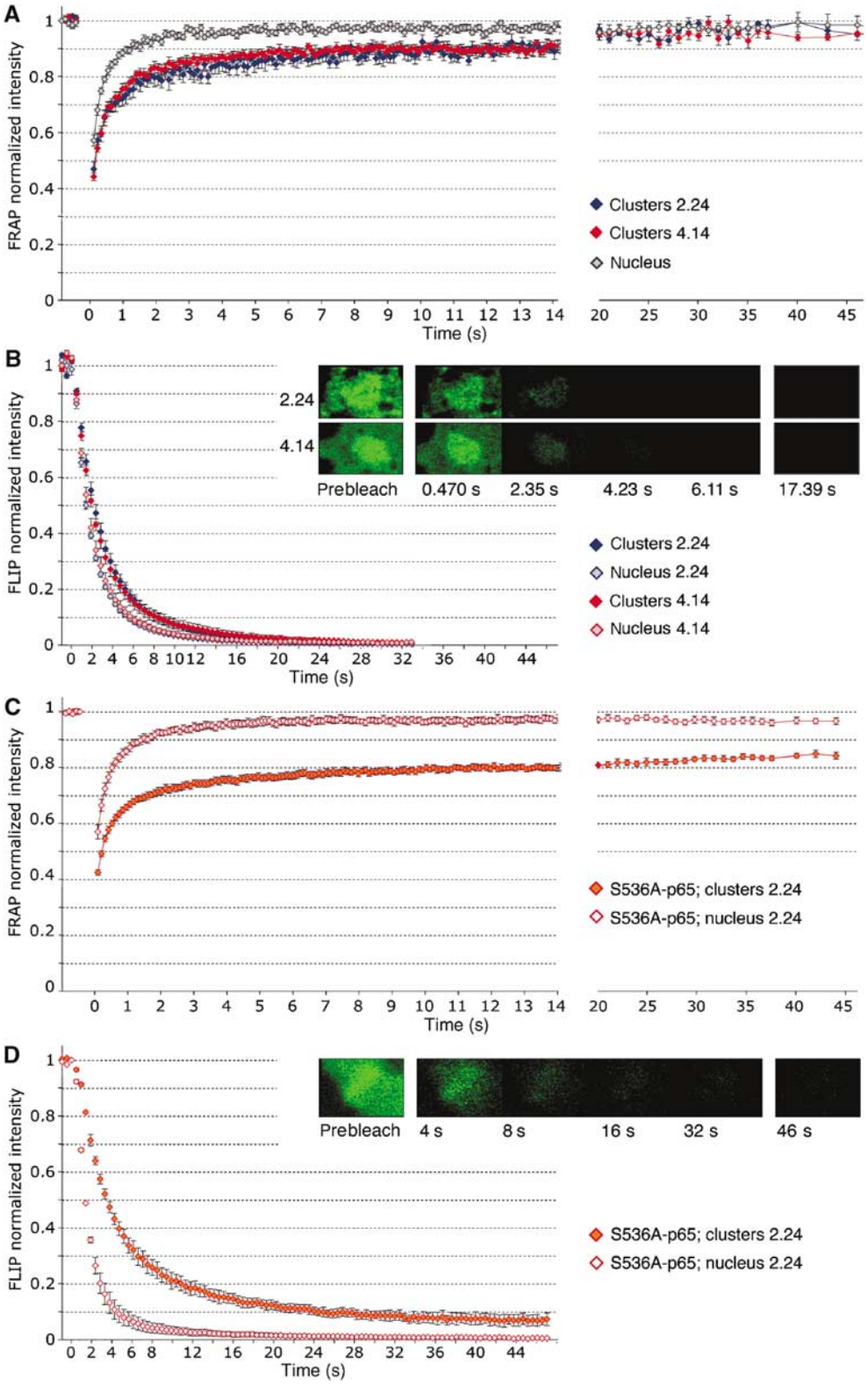

Figure 4 Dynamics of NF-κB exchange on trascriptionally active chromatin. FRAP (**A**) and FLIP (**B**) curves on clone 2.24 (HIV-LTR) and 4.14 (synthetic gene). Curves are averaged from 10 clusters per type, and 20 nondescript areas in the nuclei (the two types of clones have been merged as there is no statistical difference between them). Bars represent standard error. The differences between the curves representing the two types of clusters are statistically nonsignificant, whereas the difference between any of the clusters and the rest of the nucleus is highly significant ($P<0.001$). In (B), the image series show the fluorescence loss over time at the cluster from one cell each of clones 2.24 and 4.14. FLIP curves are averaged from 10 cells each; bars represent standard error. The differences between the curves representing the two types of clusters are statistically nonsignificant, whereas the difference between any of the clusters and the rest of the nucleus is highly significant ($P<0.002$). (**C**) FRAP and (**D**) FLIP for S536A p65-GFP on the HIV-LTR cluster (clone 2.24). Curves are averaged from eight clusters and 10 nondescript areas in the nuclei; bars represent standard error.

rate of loss from the control area (Figure 4B), demonstrating (in agreement with FRAP data) that NF-κB molecules spend a longer time on the cluster containing the HIV-1 LTR than in nondescript areas of the nucleus. However, all or nearly all NF-κB fluorescence was lost both from the array and the control area, suggesting that NF-κB molecules are not stably engaged with their sites. The experimental error does not allow us to formally and conclusively rule out the existence of an immobile fraction; however, similar to what we found for the array of κB sites (Supplementary Figure S3), if an immobile fraction exists it must be smaller than 2% (data not shown).

We also generated a second cell line (4.14) with an array of about 900 copies of a gene unit containing a synthetic NF-κB-regulated promoter (with three κB sites upstream of a minimal SV-40 promoter) driving the expression of a luciferase reporter (Figure 3A, B and D, right). Remarkably, results were indistinguishable from those obtained with the HIV-LTR (Figure 4A and B). Therefore, the kinetics of NF-κB exchange on transcriptionally active chromatin was similar in two completely unrelated gene arrays.

These results indicate that NF-κB interactions with target genes last a few seconds; as a consequence, the NF-κB-dependent events leading to transcriptional activation must take place on a similar timescale.

Active removal of NF-κB from chromatin

Such a fast exchange can be explained by at least two types of mechanisms. First, as NF-κB interaction with DNA is extremely salt-sensitive (Phelps *et al*, 2000), the exchange might occur spontaneously at the relatively high salt concentration in the cell (170 mM). The second possibility is that rapid exchange is active and catalyzed at least in part by nucleosome remodeling and proteasomal degradation, as demonstrated for GR recycling (Fletcher *et al*, 2002; Nagaich *et al*, 2004; Stavreva *et al*, 2004; Agresti *et al*, 2005). To directly address this point, we employed a p65 mutant (S536A) showing severely impaired signal-induced proteasomal degradation (Lawrence *et al*, 2005). FRAP recovery curves of S536A-p65-GFP clearly showed a large fraction of residual fluorescence on the clusters of HIV LTR even after 45 s; a similar result was obtained by FLIP (Figure 4C and D). These results demonstrate that NF-κB can reside for longer times on active genes, if its turnover is not catalyzed.

A dynamic equilibrium between promoter-bound and nucleoplasmic NF-κB

A prediction of the kinetic microscopy data is that NF-κB bound to target promoters should be in dynamic equilibrium with nucleoplasmic NF-κB molecules: if promoters are freely accessible, any change in nuclear abundance of NF-κB should cause an immediate and comparable change in target gene occupancy. To test this prediction, we used a quantitative ChIP assay to measure NF-κB recruitment to endogenous promoters in a cellular system in which NF-κB nuclear levels oscillate over time because of the rapid sequence of activation events (degradation of the IκBs and nuclear import) and negative feedback mechanisms (IκBα resynthesis) (Hoffmann *et al*, 2002).

In Raw264.7 murine macrophages, TNF-α and LPS induced different patterns of NF-κB oscillations (Figure 5A and B) that

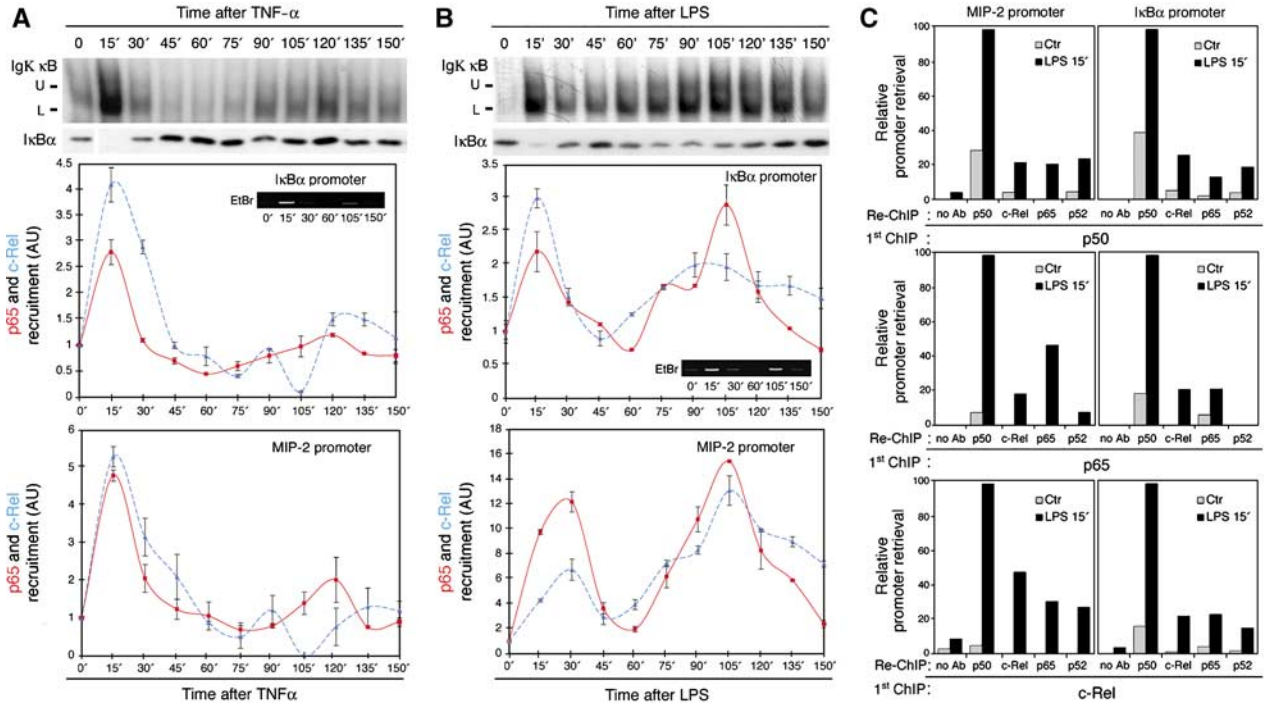

Figure 5 Pulses of NF-κB activity and recruitment of NF-κB to target genes. (**A, B**) Upper panels: EMSAs showing NF-κB activity in TNF-α- and LPS-stimulated Raw264.7 cells, respectively. A canonical κB site was used as a probe. Kinetics of IκBα degradation and resynthesis are shown. Lower panels: ChIP assays were carried out with an anti-p65 (red) or an anti-c-Rel (light blue) antibody, and recruitment to the IκBα or MIP-2 genes was measured by Q-PCR. Conventional ChIPs migrated on EtBr-stained gels are shown in small insets. Data are from a duplicate experiment and are representative of three independent experiments with similar results. (**C**) Re-ChIPs were carried out using the indicated antibodies on unstimulated and LPS-stimulated (15′) Raw264.7 cell extracts. The chromatin immunoprecipitated in the first ChIP was divided into five aliquots and re-precipitated as indicated.

were detected by electrophoretic mobility shift assays (EMSA) carried out with a canonical κB site as a probe (5′-GGGACTTTCC-3′). TNF-α induced a rapid and short pulse of NF-κB activity, followed by two additional pulses (peaking at about 120′ and 195′; Figure 5A, upper panel and data not shown). LPS-induced pulses were wider than those induced by TNF (Figure 5B, upper panel). Downregulation of NF-κB activity after the first pulse was less complete than with TNF-α; the second pulse of LPS-induced NF-κB activity was comparable in amplitude to the first one and was associated with a detectable simultaneous reduction in IκBα steady-state levels (Figure 5B).

NF-κB activity induced by both stimuli comprised the typical p50/p65 dimer and the p65/c-Rel heterodimer, which in many cell types is as abundant as p50/p65 (Hansen *et al*, 1994) and is best detected using the κB site from the human urokinase plasminogen activator (uPA) gene (5′-GGGAAAGTAC-3′) (Supplementary Figure S5). The contribution of other complexes (e.g. p50/c-Rel, p52/c-Rel) to NF-κB activity was quantitatively small.

In response to TNF-α stimulation, p65/RelA and c-Rel occupancy of the *IκBα* and *MIP-2* gene promoters (Figure 5A) closely resembled the profile of the bulk NF-κB activity as detected by EMSA: a high-amplitude cycle of NF-κB activity was followed by a second, low-amplitude cycle. In response to LPS stimulation, again both Rel proteins were detected onto DNA by ChIP in a manner that closely paralleled the cycles of NF-κB activity detected by EMSA (Figure 5B). Notably, the profiles of NF-κB activity induced by TNF-α and LPS were different; this indicates that the coincidence between total NF-κB activity and promoter occupancy is a causal relationship, and not a chance occurrence. Other promoters behaved identically to *MIP-2* and *IκBα* (Supplementary Figure S6).

The identity of the NF-κB dimers recruited to chromatin in response to stimulation was further investigated by Re-ChIP experiments, in which the chromatin pulled-down in the first round of immunoprecipitation was re-precipitated with an antibody directed against a different NF-κB protein. Re-ChIPs showed that at a single time point multiple NF-κB dimers were promoter associated (Figure 5C). This indicates that each pulse of NF-κB activity detected by anti-p65 or anti-c-Rel ChIP in fact represents the sum of the signals generated by multiple p65- or c-Rel-containing dimers.

These results demonstrate that NF-κB-regulated promoters are occupied in proportion to the NF-κB-binding activity available at any one time, as predicted on the basis of the kinetic microscopy data.

Recruitment profile of partner TFs to NF-κB-dependent genes

A second prediction of the kinetic microscopy data is that NF-κB should not generate *stable* enhanceosomes composed of NF-κB and partner TFs bound to target promoters in a cooperative fashion. If stable enhancesomes existed, removal of NF-κB from target genes at the end of the first occupancy cycle detected by ChIP should be accompanied by the simultaneous removal of partner TFs (i.e. by the disassembly of the whole enhanceosome).

To address this issue, we analyzed recruitment of multiple TFs to the canonical, rapidly activated, NF-κB-dependent *MIP-2* gene. The *MIP-2* gene promoter contains an AP-1/CRE site adjacent to the distal κB site (Figure 6A) and a C/EBP site immediately downstream of the proximal κB site. In Raw 264.7 cells, LPS stimulation induced a sustained c-Jun amino-terminal phosphorylation and an increase in c-Jun levels, whereas TNF-α stimulation did not (Figure 6A). LPS induced a sustained occupancy of the *MIP-2* promoter by c-Jun (Figure 6B). Remarkably, the c-Jun association profile with *MIP-2* was completely different from that of p65/RelA and c-Rel; in particular, c-Jun did not show any cyclic behavior and was detected at the *MIP-2* promoter between the two cycles of NF-κB recruitment (Figure 6B). We next analyzed the recruitment to the *MIP-2* promoter of additional CRE/AP-1-binding proteins (Jun B and ATF-3) and of C/EBPβ. *MIP2* gene occupancy by JunB and ATF-3 (Figure 6D) paralleled the increase in their nuclear concentration induced by LPS stimulation (Figure 6C). Nuclear levels of C/EBPβ did not change within this time frame (Figure 6C), but it was anyway efficiently recruited (Figure 6D). In all cases, these TFs displayed occupancy profiles different from those of NF-κB and could be detected at the promoter irrespective of NF-κB occupancy.

Analysis of a slow-induced gene (*Rantes/Ccl5*) showed that p65 was recruited only during the second cycle of NF-κB nuclear accumulation, whereas c-Jun, JunB and C/EBPβ occupied the promoter already at early time points (Supplementary Figure S7).

Therefore, NF-κB and partner TFs do not associate with, and are not released from target promoters as a single and stable complex.

Histone acetylation patterns at NF-κB-dependent genes are dynamical but not cyclical

NF-κB has been reported to interact with histone acetyltransferases and to mediate their recruitment to chromatin (Perkins *et al*, 1997; Zhong *et al*, 1998; Sheppard *et al*, 1999). Because estrogen receptor cycling on the *pS2* gene promoter is associated with cyclical changes in histone H3 and H4 acetylation levels (Metivier *et al*, 2003), we asked whether the cycles of NF-κB recruitment we observed are paralleled by corresponding changes in histone acetylation.

Both *MIP-2* and *IκBα* promoters are associated with relatively high basal levels of histone acetylation (Saccani *et al*, 2001). Quantitative ChIP showed a sharp peak of histone H4 and H3 hyperacetylation of *MIP-2* promoter (about three-fold increase) at 15′, followed by a rapid restoration of the initial acetylation levels that preceded NF-κB release (Figure 6E, left). The second phase of NF-κB recruitment was not associated with any detectable change in histone acetylation. At the *IκBα* gene promoter initial NF-κB recruitment was associated with a more than five-fold decrease in H3 and H4 acetylation (Figure 6E, middle); as total IκBα-associated H3 and H4 levels were not changed upon stimulation (Figure 6E, right and data not shown), the drop in acetylation detected by ChIP was mainly due to histone deacetylation, possibly mediated by recruitment of p65-associated histone deacetylases (Ashburner *et al*, 2001).

Overall, changes in histone acetylation at *MIP-2* and *IκBα* gene promoters are dissociated from the cyclic changes in NF-κB occupancy.

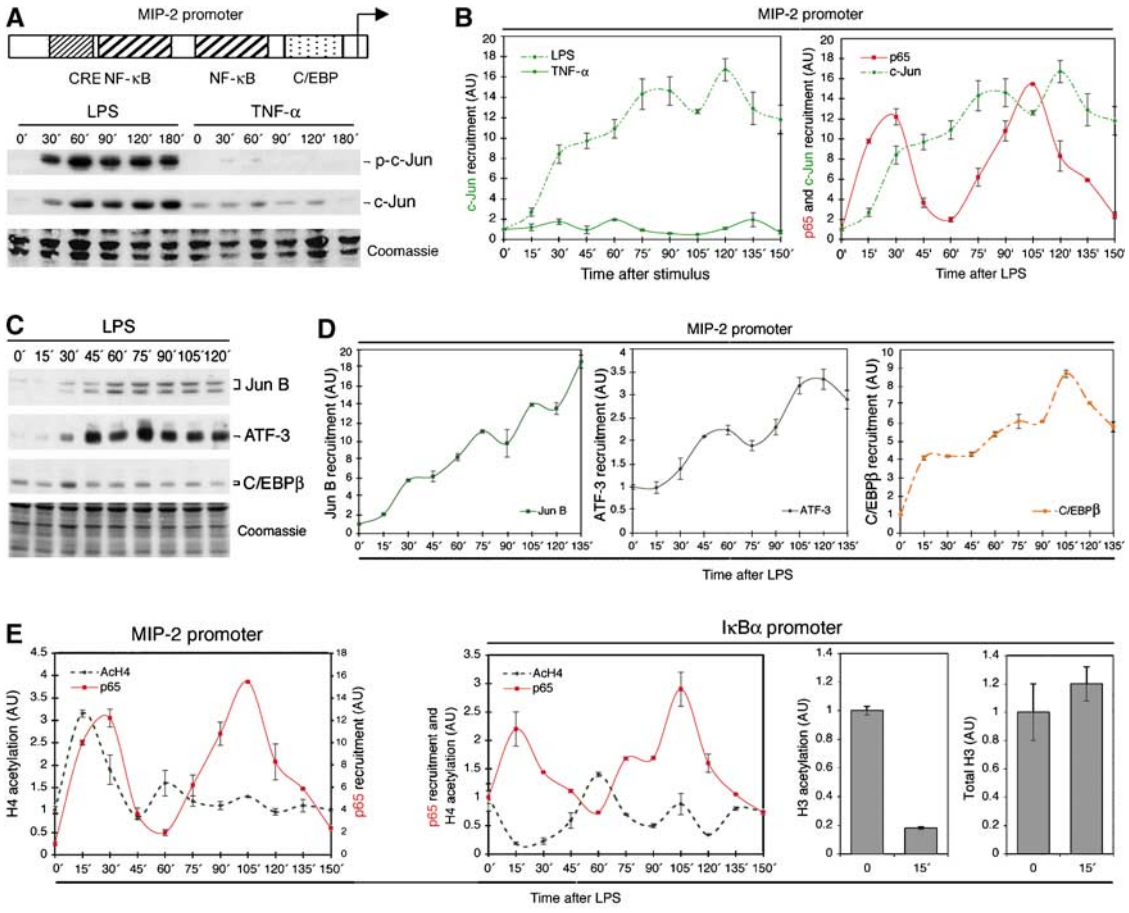

Figure 6 Recruitment of partner TFs to the MIP-2 gene promoter is dissociated from NF-κB occupancy. (**A**) Relative position of the κB, CRE and C/EBP sites in the MIP-2 promoter. Immunoblots of LPS and TNF-stimulated cells were probed with antibodies to phospho-Ser63 c-Jun or total c-Jun. A Coomassie staining of the filter is also shown. (**B**) Anti-c-Jun ChIPs in LPS and TNF-stimulated Raw264.7 cells. An overlay of p65/RelA (red) and c-Jun (green) recruitment curves in cells stimulated with LPS is shown on the right. (**C**) Immunoblots of LPS-stimulated Raw264.7 cells were probed with antibodies to JunB, ATF-3 or C/EBPβ. (**D**) Kinetics of JunB (left), ATF-3 (middle) and C/EBPβ (right) recruitment to the MIP2 promoter in LPS-stimulated Raw264.7 cells were assayed by ChIP followed by real-time PCR. (**E**) Dynamics of histone H4 acetylation (black) and p65 recruitment profiles (red) at the MIP-2 (left) and IκBα (right) gene promoters in LPS-stimulated Raw264.7 cells. Acetylated and total H3 levels are also shown.

Cyclic transcriptional activity at NF-κB-dependent genes

To determine how the recruitment profiles of NF-κB and partner TFs to target genes translate into changes in their transcriptional activity, we analyzed RNA Pol II recruitment using a ChIP assay with an antibody recognizing the RNA Pol II large subunit, rpbI. RNA Pol II association with the *IκBα* promoter increased in a cyclic fashion that closely matched the profile of p65/RelA and c-Rel occupancy (Figure 7A). Elongating RNA Pol II was also found to be present on an internal region (intron I) of the *IκBα* gene in a biphasic fashion (Figure 7A, right). The delay between maximal promoter occupancy by NF-κB and maximal RNA Pol II elongation in the second phase likely reflects the time needed by newly engaged RNA Pol II molecules to reach the intronic region detected by the probe. A similar cyclic RNA Pol II recruitment profile was detected at the *MIP-2* gene (Figure 7B), thus indicating that each cycle of NF-κB occupancy of the target promoters is associated with active transcription, while TFs occupying the promoter between the two NF-κB pulses are not sufficient to prevent transcription shutdown. Although transcriptional activity is cyclic, steady-state *MIP-2* and *IκBα* mRNA levels did not show parallel fluctuations and tended to accumulate during time (Figure 7C), indicating that the stability of these mRNAs buffers the effects of cyclic transcription. Finally, a similar correspondence between p65/RelA and RNA Pol II recruitment profiles was found at the *IκBα* and *MIP-2* promoters in response to TNF-α stimulation (Figure 7D).

Discussion

The transient nature of NF-κB:κB site interaction

Our kinetic microscopy analysis indicates that sequence-specific interactions of NF-κB with κB sites *in vivo* occur on a much faster timescale than expected from *in vitro* measurements. Three types of experiments with an increasing level of complexity and significance were carried out to analyze NF-κB mobility in the nucleus, on arrayed κB sites, and finally on transcriptionally active gene units.

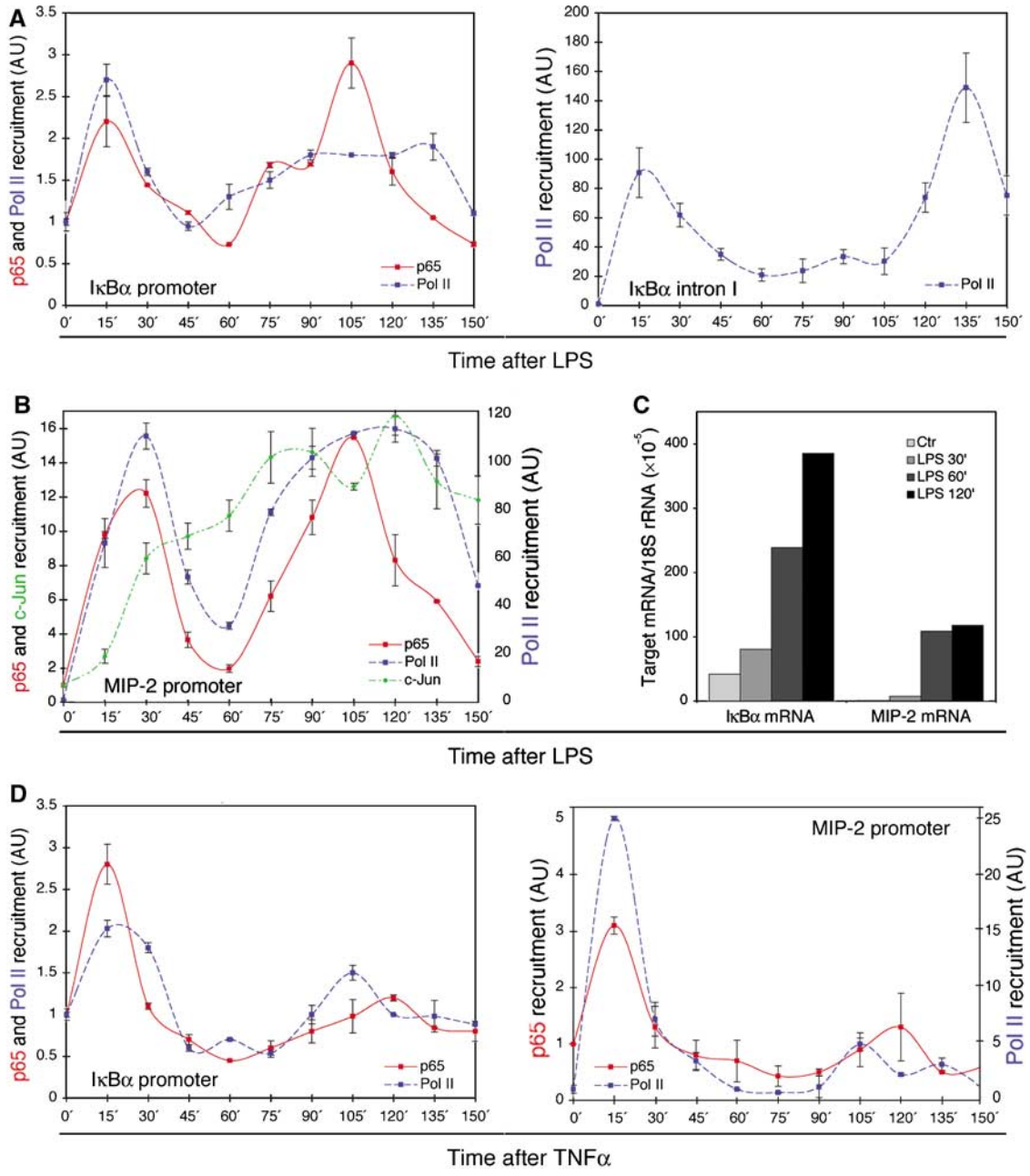

Figure 7 Cycles of transcriptional activity parallel NF-κB recruitment pulses. (**A**) RNA Pol II recruitment to the IκBα gene promoter and intron 1 was assayed by anti-rpbI ChIP on extracts from LPS-stimulated Raw264.7 cells. p65 (red) and rpb1 (blue) recruitment curves on the IκBα promoter are overlaid (left). Please note *y*-axis scale differences. (**B**) RNA Pol II recruitment to the MIP-2 promoter. Curves were overlaid with p65 (red) and c-Jun (green) recruitment curves. (**C**) Quantitative mRNA analysis of IκBα and MIP-2 transcripts. (**D**) Kinetics of RNA Pol II recruitment (blue) to the IκBα and the MIP-2 promoters in TNF-stimulated cells, and overlay with the p65 recruitment curve (red).

FRAP experiments showed that the *average* nuclear mobility of p65/RelA was comparable or even faster than that of GR. This was further corroborated by the direct *in vivo* visualization of NF-κB exchange on κB sites contained within chromatinized, stably integrated arrays. Again, NF-κB was found to very rapidly exchange between the array and the rest of the nucleus. On active genes there was a transient but measurable immobilization of p65; nevertheless, the mobility was still very high and exchange complete or nearly complete.

Because active transcription and fast NF-κB exchange coexist, it can be concluded that preinitiation complex assembly and transcriptional activation do not require (and are not associated with) stable interactions of NF-κB with cognate sites. On the other hand, the transient immobilization of NF-κB on chromatin upon interaction with specific sites in active promoters likely represents a critical step in NF-κB-dependent gene induction: NF-κB residence time on specific sites defines a *stochastic window* during which general TFs (and possibly additional sequence specific TFs essential for activation) must collide with the same regulatory region for transcription to occur.

The removal of NF-κB from κB sites appears to be active and catalyzed, as a single-site mutation that

impairs proteasomal degradation of p65 (Lawrence *et al*, 2005) can considerably extend its residence time on active genes.

A dynamic equilibrium between promoter-bound and nucleoplasmic NF-κB

The first implication of the rapid exchange of NF-κB between chromatin and the nucleoplasmic compartment is that maintenance of κB site occupancy will require the continuous supply of NF-κB dimers. Therefore, any oscillation in NF-κB nuclear levels will immediately reverberate on NF-κB occupancy of target genes, and any change in the abundance of different NF-κB dimers will cause a change in the relative representation of the NF-κB dimers bound to κB site-containing promoters ('dimer exchange', see Saccani *et al*, 2003). In other words, promoter-bound NF-κB is at equilibrium with its nucleoplasmic pool.

What is the relationship between the pulses of NF-κB recruitment to target genes detected by ChIP (i.e. pulses measurable on a timescale of tens of minutes) and the very fast exchange of NF-κB between target sites and nucleoplasm (i.e. an exchange measurable on a timescale of seconds)? And are the results obtained with the two techniques in conflict with each other?

If NF-κB:DNA complexes lasted tens of minutes, as suggested by the *in vitro* results (Zabel and Baeuerle, 1990), ChIP would detect a corresponding pulse of NF-κB association with target promoters, which is in fact the result we obtained. However, if the NF-κB:DNA complexes were short lasting, as suggested by the kinetic microscopy analysis, the results of the ChIP assay would be exactly the same. Indeed, formaldehyde handcuffs TFs on chromatin thus preserving labile and transient interactions and providing an *average* of the promoter occupancy status in the cell population *at a given moment*: a low degree of occupancy will be found when nuclear NF-κB levels are low and a high degree when nuclear levels are maximal, even if exchange in living cells (in the absence of formaldehyde) is very fast. In fact, ChIP does not provide any kinetic information on the *duration* of TF–DNA interactions, while kinetic microscopy does: when kinetics of NF-κB exchange (analyzed by FLIP or FRAP) and promoter occupancy (analyzed by ChIP) are assayed on the same chromatin target (HIV-CFP-SKL array in clone 2.24), it becomes obvious that a hyper-dynamic exchange underlies the apparently steady interaction of NF-κB with DNA revealed by ChIP.

Finally, the fact that multiple NF-κB dimers are simultaneously detected at target genes using Re-ChIP is consistent with the idea that all the dimers available in the nucleus at any given time point may transiently collide with the promoter with a frequency that mainly reflects their nuclear abundance (i.e. following probabilistic rules).

Revising the enhanceosome concept in a dynamic framework

The multiprotein complex of NF-κB, companion TFs and architectural proteins bound to the *IFN*-β enhancer is the paradigm of enhanceosomes (Thanos and Maniatis, 1995b; Carey, 1998; Maniatis *et al*, 1998; Merika and Thanos, 2001). Other enhanceosomes containing NF-κB as an essential component have also been described (Whitley *et al*, 1994; Vanden Berghe *et al*, 1999). Enhanceosomes are supposed to be extremely stable (Yie *et al*, 1999), a concept that is obviously in contrast with the fast mobility of NF-κB on its cognate sites that we demonstrate here. Can we reconcile the apparently long-term existence of enhanceosomes with the short-term residence of NF-κB on DNA? We envision two possible scenarios. The first is simply that enhanceosomes form very fast and completely disassemble very fast, only to perform again a new, complete and fast assembly cycle. In this way, enhanceosomes would be present on average on enhancers, and thus may appear stable if assayed by ChIP in a population of cells, whereas they would appear extremely dynamic if individually analyzed. The second possibility is that enhanceosomes, as an assembly of multiple proteins species, are indeed stable; however, a given protein species in the enhanceosome would be in dynamic equilibrium with soluble molecules of the same species. In this interpretation, partially complete enhanceosomes would bind a specific molecule and become complete, only to lose another component molecule seconds later. Partially complete enhanceosomes would probably be the majority, but a formal demonstration of their existence may not be obtained by ChIP. Our data on the clusters of active genes do not allow us to formally exclude a third possibility, namely that a very small fraction of stable enhanceosomes exists that accounts for all transcriptional activity. However, we find this possibility very unlikely, given the substantial amount of RNA polymerase recruited to the clusters and its extensive colocalization with p65: both findings are difficult to reconcile with an extreme minority of active enhanceosomes.

The enhanceosome model also postulates that all TFs participate in enhanceosome assembly and thus are *equally relevant*: knock-down of any of them will result in loss of function (Thanos and Maniatis, 1995b). Conversely, our data indicate the existence of an obvious *hierarchy*, in which NF-κB dominates in promoting RNA Pol II recruitment and gene transcription. In fact, a drop in gene-bound RNA-Pol II accompanies any decay in NF-κB occupancy, thus suggesting that partner TFs (AP1, C/EBPβ and others) may serve accessory roles not directly related to RNA-Pol II recruitment. Related to this point is the occupancy of the *MIP-2* promoter by NF-κB and partner TFs. ChIP data indicate that AP-1 and C/EBP proteins have different occupancy profiles as compared to NF-κB, and that apparently they remain promoter-bound between the two cycles of NF-κB occupancy.

Overall, our data suggest that NF-κB and partner TFs associate with and dissociate from promoters quickly and largely independently from each other, and not as a single and highly stable complex. In fact, it is absolutely likely that all TFs are rapidly exchanging with chromatin on a timescale of seconds (Misteli, 2001; Phair *et al*, 2004a). In this light, any *slow* change (increase or decay) in promoter occupancy detected by ChIP (i.e. a change occurring on a timescale of minutes) can be interpreted as a direct consequence of a change in the equilibrium levels of each TF, whose rapid update relies on the *fast* association–dissociation cycles detected by kinetic microscopy.

A biological perspective

The *transient immobilization* of NF-κB on chromatin intuitively represents the best compromise between two essential

and in part contrasting needs: the need to maximize the chances of a productive encounter with the transcriptional machinery; and the need to prevent the sequestration of NF-κB on the many thousand κB sites occurring in the genome. Moreover, rapid release from cognate sites grants that changes in the nuclear abundance of NF-κB dimers will be immediately 'sensed' by the target promoter, thus leading to a corresponding change in occupancy and transcriptional activity. In fact, the nuclear concentration of NF-κB will be sampled hundreds of times within a single NF-κB activation cycle, which allows promoters to quickly re-tune their activity as external conditions change. Such oversampling is possibly overkill for enabling the slow cycles observed under cell culture conditions, and an intriguing possibility is that rapid exchange may serve other purposes as well. However, real cells in real life might experience much more rapidly changing conditions that require mechanisms enabling a very fast adaptation. NF-κB-driven transcription occurs within minutes after stimulation and mediates a quick adaptation to a stressful situation, be it the encounter with a pathogen, the exposure to radiations or the release of inflammatory cytokines. As such, the transcriptional status of NF-κB-activated genes must be quickly re-tuned. To the contrary, the enhanceosome is supposed to be such a stable structure to be poorly responsive to environmental changes: once formed it reacts poorly (if at all) to changes in the external conditions that provoked its formation. Although the specific transcriptional needs of selected genes with very complex requirements (like the *IFN*-β gene) (Maniatis *et al*, 1998) and/or sustained transcriptional activity (like the *TCR* α-chain gene) (Giese *et al*, 1995) may be best met by the assembly of stable enhanceosomes, our data strongly suggest that transcription of most NF-κB-dependent genes (that are rapidly and transiently induced) occurs via hyperdynamic interactions.

Materials and methods

Antibodies

The following antibodies were obtained from Santa Cruz Biotechnology: anti-p65 sc-372; anti-c-Rel sc-71; anti-p52 sc-298; anti-c-Jun sc-1694; anti-JunB sc-8051; anti-ATF3 sc-188; anti-C/EBPβ sc-150; anti rpbI sc-899. The anti-Ac-histone H3 (#06–599) and the anti-Ac H4 (#06–866) antisera were from Upstate Biotechnology Inc. The anti-H3 antibody (9712) and the anti-phospho Ser63 c-Jun antibody (9261) were from Cell Signaling Technology and the anti-p50 ab7971 from Abcam.

Electrophoretic mobility shift assay

EMSAs were performed as described (Saccani *et al*, 2001). The probes used were: κB 5′-AGTTGAGGGGACTTTCCCAGGC-3′ and hum uPA κB 5′-GCTGCCTGCTGGGGAAAGTAC-3′.

Chromatin immunoprecipitation assays

ChIP assays were carried out as described (Saccani *et al*, 2001) with minor modifications (protocol is available upon request).

Wide-field imaging

Colocalization of GFP-pol II and mRFP-p65 was analyzed in living cells from clones 2.24 and 4.14 as described in Agresti *et al* (2005). The images (20 per cell) were spaced by 0.1 μm on the *z*-axis.

Confocal imaging

Stacks of images were acquired at 37°C on a Leica TCS SP2 AOBS confocal microscope with a × 63/1.4 NA oil immersion objective and × 6 zoom (512 × 512 pixels; voxel size 0.077 × 0.077 × 0.1 μm).

In vivo kinetic microscopy

HeLa cells were transfected with FuGene (Roche) with concentrations of GFP-p65/RelA expression vector optimized to achieve expression levels comparable to or lower than the endogenous protein. Cells were stimulated with TNF-α for 20 min before FRAP. FRAP was as described in Agresti *et al* (2005), except that zoom was × 6. Bleaching was performed on areas of radius 1 μm (Figure 1) or 0.75 μm (Figures 2 and 4).

FLIP experiments were performed with the same confocal microscope, with × 6 zoom at 470 ms per frame. Cells from clones 2.24 and 4.14 were transfected with p65-GFP and untagged p50 and stimulated for 20 min with TNF-α. Each experiment was repeated at least twice. Three 12-bit prebleaching frames were acquired with the 488 nm line at 10% of the maximal power. Repetitive bleaching was performed using FRAP settings on about 90% of the nucleus area, whereas simultaneously imaging the untargeted area (same settings as for prebleaching).

Array of κB sites

The κB-384 construct was generated using the strategy of Robinett *et al* (1996). The sequence of the basic unit containing three canonical κB sites (underlined) was: 5′-GATCCCTCGAGGG GACTTTCCGCTAGGGACTTTCCGCTAGGGACTTTCCG-3′. This unit was cloned in pUC19 by *Bam*HI/*Sal*I and sequentially doubled in seven identical cloning steps to reach 128 copies. The resultant κB-384 plasmid was cotransfected with pBabe-Puro in HeLa cells in a 20:1 ratio; single clones were picked after 12 days of selection with 1 μg/ml puromycin. Clones were screened for the presence of the array by PCR; positive clones were further screened by GFP-p65 + p50 cotransfection and direct visualization of the array. Two clones (11 and 16) showing a single bright spot in most cells were selected for FRAP experiments.

Clones were transfected and stimulated as above. Stacks of 20 images centered on the bright fluorescent cluster of κB sites were acquired at 37°C with a × 60/1.4 NA oil immersion objective and × 6 zoom as described.

NF-κB-regulated gene arrays

The hygromycin resistance cassette in pSFV-dhfr (Shimizu *et al*, 2001) was excised by *Nru*I–*Bam*HI and replaced by a gene unit in which a 720 bp *Hin*dIII–*Xho*I fragment of the HIV1-LTR (from plasmid pHIV-CAT) (Nabel and Baltimore, 1987) drives the expression of a CFP variant bearing a C-terminal SKL tripeptide. The resulting plasmid, SFV-dhfr-HIV-LTR(CFP-SKL) was transfected into immortalized p65-p50 double knock-out mouse fibroblasts (a gift from K Marcu, SUNY at Stony Brook) and stable clones bearing amplified plasmid sequences were obtained by blasticidin selection (Shimizu *et al*, 2001, 2003). Clones were analyzed by Q-PCR using primers amplifying both the Chinese hamster DHFR genomic region contained in pSFV-dhfr and the endogenous mouse counterpart (Oriβ For: 5′-GCCTTAACCTTTGTTCTGTAAATG-3′; ORIβ Back: 5′-GAGGCCATCTRTGRAGCTGCTG-3′). Copy number was estimated by comparing the Ct of the parental cells with those of individual clones. Stable clones bearing an amplified κB-luc gene unit were obtained by cotransfection of equimolar amounts of p3X-κB-luc and a pSFV-dhfr derivative (pΔBN-AR1) that efficiently promotes amplification of cotransfected plasmids (Shimizu *et al*, 2003).

The plasmid expressing a GFP-tagged rpb1 subunit of RNA Pol II was a kind gift of M Vigneron and K Sugaya (Sugaya *et al*, 2000). The mRFP-p65 vector was obtained by replacing the GFP coding sequence of hup65-GFP (Saccani *et al*, 2004) with the *Hin*dIII–*Bam*HI fragment of pRSET-mRFP1 (Campbell *et al*, 2002). pRK-p65 S536A was a kind gift of T Lawrence and M Karin: the fragment containing the mutated amino acid was PCR amplified and used to replace the corresponding sequence in p65-GFP.

Statistical analysis

Statistical analysis was performed with the Prism 4 (GraphPad) using two-way analysis of variance.

Supplementary data

Supplementary data are available at *The EMBO Journal* Online.

Acknowledgements

We thank G Verde (San Raffaele Scientific Institute) for unpublished results, and GM Wahl (Salk Institute, La Jolla), M Vigneron (INSERM, Strasbourg, France), K Sugaya (NIRS, Chiba, Japan), K Marcu (SUNY at Stony Brook), T Lawrence and M Karin for gifts of reagents. pHIV-CAT (from Dr G Nabel and Dr N Perkins) was obtained through the AIDS Research and Reference Reagent Program, NIAID, NIH. This work was supported by grants from the Swiss National Science Foundation and Oncosuisse to GN and from Ministero dell'Istruzione, Università e Ricerca to AA and MEB. DB was supported by a Roche Research Foundation fellowship. *Author contributions*. DB: experimental design and execution of the ChIP assays; IM: EMSAs and generation of the array constructs and cell lines; AA: design, execution and analysis of all the FRAP and FLIP experiments; NS: help with the generation of transcribed arrays; MB: FRAP and FLIP design and analysis and paper writing; GN: experimental design, generation of transcribed arrays, and paper writing.

References

Agresti A, Scaffidi P, Riva A, Caiolfa VR, Bianchi ME (2005) GR and HMGB1 interact only within chromatin and influence each other's residence time. *Mol Cell* **18:** 109–121

Ashburner BP, Westerheide SD, Baldwin Jr AS (2001) The p65 (RelA) subunit of NF-κB interacts with the histone deacetylase (HDAC) corepressors HDAC1 and HDAC2 to negatively regulate gene expression. *Mol Cell Biol* **21:** 7065–7077

Bonaldi T, Talamo F, Scaffidi P, Ferrera D, Porto A, Bachi A, Rubartelli A, Agresti A, Bianchi ME (2003) Monocytic cells hyperacetylate chromatin protein HMGB1 to redirect it towards secretion. *EMBO J* **22:** 5551–5560

Campbell RE, Tour O, Palmer AE, Steinbach PA, Baird GS, Zacharias DA, Tsien RY (2002) A monomeric red fluorescent protein. *Proc Natl Acad Sci USA* **99:** 7877–7882

Carey M (1998) The enhanceosome and transcriptional synergy. *Cell* **92:** 5–8

Chen-Park FE, Huang DB, Noro B, Thanos D, Ghosh G (2002) The kappa B DNA sequence from the HIV long terminal repeat functions as an allosteric regulator of HIV transcription. *J Biol Chem* **277:** 24701–24708

Fletcher TM, Xiao N, Mautino G, Baumann CT, Wolford R, Warren BS, Hager GL (2002) ATP-dependent mobilization of the glucocorticoid receptor during chromatin remodeling. *Mol Cell Biol* **22:** 3255–3263

Ghosh S, May MJ, Kopp EB (1998) NF-kappa B and Rel proteins: evolutionarily conserved mediators of immune responses. *Annu Rev Immunol* **16:** 225–260

Giese K, Kingsley C, Kirshner JR, Grosschedl R (1995) Assembly and function of a TCR alpha enhancer complex is dependent on LEF-1-induced DNA binding and multiple protein–protein interactions. *Genes Dev* **9:** 995–1008

Hansen SK, Baeuerle PA, Blasi F (1994) Purification, reconstitution, and IκB association of the c-Rel-p65 (RelA) complex, a strong activator of transcription. *Mol Cell Biol* **14:** 2593–2603

Hoffmann A, Levchenko A, Scott ML, Baltimore D (2002) The IκB-NF-κB signaling module: temporal control and selective gene activation. *Science* **298:** 1241–1245

Lawrence T, Bebien M, Liu GY, Nizet V, Karin M (2005) IKKα limits macrophage NF-κB activation and contributes to the resolution of inflammation. *Nature* **434:** 1138–1143

Maniatis T, Falvo JV, Kim TH, Kim TK, Lin CH, Parekh BS, Wathelet MG (1998) Structure and function of the interferon-β enhanceosome. *Cold Spring Harb Symp Quant Biol* **63:** 609–620

Martone R, Euskirchen G, Bertone P, Hartman S, Royce TE, Luscombe NM, Rinn JL, Nelson FK, Miller P, Gerstein M, Weissman S, Snyder M (2003) Distribution of NF-κB-binding sites across human chromosome 22. *Proc Natl Acad Sci USA* **100:** 12247–12252

McNally JG, Muller WG, Walker D, Wolford R, Hager GL (2000) The glucocorticoid receptor: rapid exchange with regulatory sites in living cells. *Science* **287:** 1262–1265

Merika M, Thanos D (2001) Enhanceosomes. *Curr Opin Genet Dev* **11:** 205–208

Metivier R, Penot G, Hubner MR, Reid G, Brand H, Kos M, Gannon F (2003) Estrogen receptor-α directs ordered, cyclical, and combinatorial recruitment of cofactors on a natural target promoter. *Cell* **115:** 751–763

Misteli T (2001) Protein dynamics: implications for nuclear architecture and gene expression. *Science* **291:** 843–847

Muller WG, Rieder D, Kreth G, Cremer C, Trajanoski Z, McNally JG (2004) Generic features of tertiary chromatin structure as detected in natural chromosomes. *Mol Cell Biol* **24:** 9359–9370

Nabel G, Baltimore D (1987) An inducible transcription factor activates expression of human immunodeficiency virus in T cells. *Nature* **326:** 711–713

Nagaich AK, Walker DA, Wolford R, Hager GL (2004) Rapid periodic binding and displacement of the glucocorticoid receptor during chromatin remodeling. *Mol Cell* **14:** 163–174

Natoli G, Saccani S, Bosisio D, Marazzi I (2005) Interactions of NF-κB with chromatin: the art of being at the right place at the right time. *Nat Immunol* **6:** 439–445

Perkins ND, Felzien LK, Betts JC, Leung K, Beach DH, Nabel GJ (1997) Regulation of NF-κB by cyclin-dependent kinases associated with the p300 coactivator. *Science* **275:** 523–527

Phair RD, Gorski SA, Misteli T (2004a) Measurement of dynamic protein binding to chromatin *in vivo*, using photobleaching microscopy. *Methods Enzymol* **375:** 393–414

Phair RD, Scaffidi P, Elbi C, Vecerova J, Dey A, Ozato K, Brown DT, Hager GL, Bustin M, Misteli T (2004b) Global nature of dynamic protein–chromatin interactions *in vivo*: three-dimensional genome scanning and dynamic interaction networks of chromatin proteins. *Mol Cell Biol* **24:** 6393–6402

Phelps CB, Sengchanthalangsy LL, Malek S, Ghosh G (2000) Mechanism of κB DNA binding by Rel/NF-κB dimers. *J Biol Chem* **275:** 24392–24399

Robinett CC, Straight A, Li G, Willhelm C, Sudlow G, Murray A, Belmont AS (1996) *In vivo* localization of DNA sequences and visualization of large-scale chromatin organization using lac operator/repressor recognition. *J Cell Biol* **135:** 1685–1700

Saccani S, Marazzi I, Beg AA, Natoli G (2004) Degradation of promoter-bound p65/RelA Is essential for the prompt termination of the NF-κB response. *J Exp Med* **200:** 107–113

Saccani S, Pantano S, Natoli G (2001) Two waves of NF-κB recruitment to target promoters. *J Exp Med* **193:** 1351–1359

Saccani S, Pantano S, Natoli G (2003) Modulation of NF-κB activity by exchange of dimers. *Mol Cell* **11:** 1563–1574

Sheppard KA, Rose DW, Haque ZK, Kurokawa R, McInerney E, Westin S, Thanos D, Rosenfeld MG, Glass CK, Collins T (1999) Transcriptional activation by NF-κB requires multiple coactivators. *Mol Cell Biol* **19:** 6367–6378

Shimizu N, Hashizume T, Shingaki K, Kawamoto JK (2003) Amplification of plasmids containing a mammalian replication initiation region is mediated by controllable conflict between replication and transcription. *Cancer Res* **63:** 5281–5290

Shimizu N, Miura Y, Sakamoto Y, Tsutsui K (2001) Plasmids with a mammalian replication origin and a matrix attachment region initiate the event similar to gene amplification. *Cancer Res* **61:** 6987–6990

Stavreva DA, Muller WG, Hager GL, Smith CL, McNally JG (2004) Rapid glucocorticoid receptor exchange at a promoter is coupled to transcription and regulated by chaperones and proteasomes. *Mol Cell Biol* **24:** 2682–2697

Sugaya K, Vigneron M, Cook PR (2000) Mammalian cell lines expressing functional RNA polymerase II tagged with the green fluorescent protein. *J Cell Sci* **113** (Part 15)**:** 2679–2683

Thanos D, Maniatis T (1995a) NF-κB: a lesson in family values. *Cell* **80:** 529–532

Thanos D, Maniatis T (1995b) Virus induction of human IFNβ gene expression requires the assembly of an enhanceosome. *Cell* **83:** 1091–1100

Urban MB, Baeuerle PA (1990) The 65-kD subunit of NF-κB is a receptor for IκB and a modulator of DNA-binding specificity. *Genes Dev* **4:** 1975–1984

Vanden Berghe W, De Bosscher K, Boone E, Plaisance S, Haegeman G (1999) The nuclear factor-κB engages CBP/p300 andhistone acetyltransferase activity for transcriptional activation of the interleukin-6 gene promoter. *J Biol Chem* **274:** 32091–32098

Verma IM, Stevenson JK, Schwarz EM, Van Antwerp D, Miyamoto S (1995) Rel/NF-κB/IκB family: intimate tales of association and dissociation. *Genes Dev* **9:** 2723–2735

Whitley MZ, Thanos D, Read MA, Maniatis T, Collins T (1994) A striking similarity in the organization of the E-selectin and β−interferon gene promoters. *Mol Cell Biol* **14:** 6464–6475

Yie J, Merika M, Munshi N, Chen G, Thanos D (1999) The role of HMG I(Y) in the assembly and function of the IFN-β enhanceosome. *EMBO J* **18:** 3074–3089

Zabel U, Baeuerle PA (1990) Purified human IκB can rapidly dissociate the complex of the NF-κB transcription factor with its cognate DNA. *Cell* **61:** 255–265

Zhong H, Voll RE, Ghosh S (1998) Phosphorylation of NF-κB p65 by PKA stimulates transcriptional activity by promoting a novel bivalent interaction with the coactivator CBP/p300. *Mol Cell* **1:** 661–671

